Dynamic Model of Basic Oxygen Steelmaking Process Based on Multizone Reaction Kinetics: Modeling of Decarburization

BAPIN KUMAR ROUT, GEOFFREY BROOKS, M. AKBAR RHAMDHANI, ZUSHU LI, FRANK N.H. SCHRAMA, and AART OVERBOSCH

In a previous study by the authors (Rout *et al.* in Metall Mater Trans B 49:537–557, 2018), a dynamic model for the BOF, employing the concept of multizone kinetics was developed. In the current study, the kinetics of decarburization reaction is investigated. The jet impact and slag–metal emulsion zones were identified to be primary zones for carbon oxidation. The dynamic parameters in the rate equation of decarburization such as residence time of metal drops in the emulsion, interfacial area evolution, initial size, and the effects of surface-active oxides have been included in the kinetic rate equation of the metal droplet. A modified mass-transfer coefficient based on the ideal Langmuir adsorption equilibrium has been proposed to take into account the surface blockage effects of SiO_2 and P_2O_5 in slag on the decarburization kinetics of a metal droplet in the emulsion. Further, a size distribution function has been included in the rate equation to evaluate the effect of droplet size on reaction kinetics. The mathematical simulation indicates that decarburization of the droplet in the emulsion is a strong function of the initial size and residence time. A modified droplet generation rate proposed previously by the authors has been used to estimate the total decarburization rate by slag–metal emulsion. The model's prediction shows that about 76 pct of total carbon is removed by reactions in the emulsion, and the remaining is removed by reactions at the jet impact zone. The predicted bath carbon by the model has been found to be in good agreement with the industrially measured data.

I. INTRODUCTION

THE refining reaction of carbon in a top blowing steelmaking process primarily takes place in the jet impact region and between metal drops and slag in the slag–metal–gas emulsion.[1] The total refining of carbon from the bath can be expressed as

$$\left(\frac{dW_c}{dt}\right)_{total} = \left(\frac{dW_c}{dt}\right)_{em} + \left(\frac{dW_c}{dt}\right)_{iz}, \qquad [1]$$

where $\left(\frac{dW_c}{dt}\right)_{total}$ is the total decarburization rate (kg/s), $\left(\frac{dW_c}{dt}\right)_{em}$ is the rate of carbon removal from the emulsion

zone (kg/s), and $\left(\frac{dW_c}{dt}\right)_{iz}$ is the rate of carbon removed from the jet impact zone (kg/s).

The importance of slag–metal emulsion on the rate of decarburization reaction has been first realized when the early researchers observed cavity and blow holes in the metal drops found in the slag sample, collected from the upper part of the furnace.[2,3] The significant low value of carbon concentration measured in the metal drop compared with metal bath further indicates that the ejected metal drops are decarburized to a large extent in the emulsion phase.[4,5] The emulsion mechanism of decarburization became evident when Mollseau and Fruehan investigated the kinetics behavior of Fe-C-S droplets in slag by X-ray fluoroscopy.[6] These authors observed that the metal drop containing carbon, when it passes through high FeO (> 10 wt pct) in slag, undergoes expansion in volume due to internal nucleation of CO bubbles. The experimentally observed value of residence time of metal drop in the emulsion is in the order of ~10 seconds, whereas the residence time of nonbloating dense drops accounts for only a fraction of a second.[7] Considerably large volume expansion decreases the density of drops and allows the decarburization reaction to proceed for a finite time in the slag–metal emulsion phase. Large interfacial

BAPIN KUMAR ROUT, GEOFFREY BROOKS, and M. AKBAR RHAMDHANI are with the Faculty of Science, Engineering and Technology, Swinburne University of Technology, Hawthorn, Victoria, 3122, Australia. Contact e-mail: brout@swin.edu.au ZUSHU LI is with the WMG, University of Warwick, Coventry CV4 7AL, UK. FRANK N.H. SCHRAMA and AART OVERBOSCH are with Tata Steel, Netherlands, 1970 CA IJmuiden, The Netherland.
Manuscript submitted June 23, 2016.
Article published online March 20, 2018.

area for reaction caused by the breakup of the bulk metal into small fragments along with ample reaction time (residence time) explains the rapid decarburization kinetics observed in a top blowing steelmaking process.

Mathematical models have been developed to simulate the phenomena of bloating and decarburization reaction kinetics of a single drop in slag.[7,8] The work resulted in the theory of ''bloated droplet'' which subsequently applied by several authors to develop overall decarburization model applicable for real converter process.[8–11] Different aspects of kinetic models available in the literature for refining of carbon in the emulsion are summarized in Table I. The successful application of the theory of swelling of drops to an industrial-scale decarburization model can be attributed to Dogan et al.[8] The authors applied the residence time model by Brooks et al.[7] and the droplet generation model suggested by Subagyo et al.[12] to calculate the overall decarburization kinetics in slag–metal emulsion zone. The model used only monosized droplets and ignored the different modes of splashing on the kinetics of the process. In a recent study Rout et al.[13] proposed a correction in the previous droplet generation rate based on jet behavior under high temperature environment and mode of splashing. Although Dogan et al.'s model provides a good explanation for the overall decarburization rate, the model failed to explain the slow rate of decarburization kinetics during the initial blowing stage and unable to give explanation for the different decarburization rates for drops of different sizes. Also, the decarburization model by Dogan et al. overestimates carbon-refining rate in the emulsion when the modified droplet generation was applied. Figure 1 demonstrates the comparison of the carbon refining by the emulsion zone based on Subagyo's model of droplet generation ($R_{B,T}$) to the one with modified formula suggested by Rout et al. In both the computations, the average size of the droplet was assumed to be 2×10^{-3} m. As seen from Figure 1, in the case of modified droplet generation, the decarburization rate predicted by Dogan's model is more rapid and exceeds the measured decarburization rate in the bath. The observed higher rate of decarburization rate is primarily due to the difference in the ejected metal drops predicted by the modified droplet generation correlation.

Several researchers reported that the size of a metal drop ejected from the melt exhibits a significant variation, and the size spectrum can be mathematically described by Rosin–Rammler–Sperling (RRS) distribution function.[12,14] Further, the examination of metal drops collected from the emulsion suggests that the kinetics of decarburization largely depend on the size of drops.[2,4,5] Chen and Coley[17] observed that all the metal droplets go through an incubation period before the swelling takes place. Those droplets which can be capable of nucleating CO bubbles before falling back to the metal phase only increase the residence time in slag–metal emulsion. Since the rate of decarburization is proportional to the reaction time (residence time), the incubation time for CO nucleation plays a significant role in determining the refining rate of droplets. Further, Chen et al. found that the incubation time is a strong function of C, S concentrations in the droplet and the level of FeO in slag.

When a metal drop is ejected into the emulsion phase, other than carbon, it contains several other impurities such as Si, Mn, P, and S, and it has been postulated that the removal of these impurities occurs simultaneously rather than sequentially. A recent study by Millman et al.[5] showed that thermodynamic equilibrium predictions might not be sufficient to explain the refining path of these impurities. The apparent deviation from equilibrium thermodynamic suggests that the process is controlled kinetically, and the simultaneous removal of C, Si, Mn, and P may be studied by a kinetically limiting approach. Several researchers reported that the retardation of decarburization rate due to the presence of Si is associated with interfacial phenomena, perhaps due to the adsorption of SiO$_2$ at surface sites.[18–20] Mulholland et al.[18] hypothesized that silica adsorbs onto the surface sites and forms a thin layer of SiO$_2$ around the drop which is responsible for inhibition of decarburization reaction. Woolley et al.[19] reported that addition of Si and P decreases the decarburization rate by the formation of viscous oxide layers at the slag–metal interface. Kim et al.[20] showed that the silica reduces the surface tension of FeO-SiO$_2$ melts and can occupy up to 70 pct of the surface sites available for FeO reduction reaction. Similarly, the firm surface-active nature of P$_2$O$_5$ has been reported by several researchers,[2,21] and the presence of P in the metal drop is responsible for retardation of decarburization rate. Wei et al.[21]

Table I. Different Aspects of Modeling of Various Parameters Relevant to Kinetics of Decarburization in Slag–Metal Emulsion (NC, Not Considered; C, Considered)

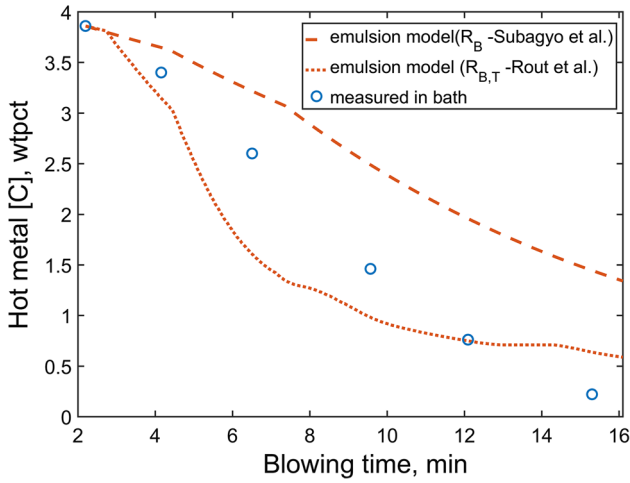| Authors	Residence Time	Kinetics (Single Drop)	Droplet Generation Rate	Size Distribution	Effect of Other Elements	Effect of Slag	Overall Kinetics Emulsion
Koria et al.,[14] Subagyo et al. [12]	NC	NC	NC	C	NC	NC	NC
Subagyo et al.,[12] He et al.,[15] Rout et al.[13]	NC	NC	C	NC	NC	NC	NC
Brooks et al.[7]	C	C	NC	NC	NC	NC	NC
Sun H.[16]	C	C	NC	NC	C	NC	NC
Chen and Coley[17]		C					
Dogan et al.[8–10]	C	C	C	NC	NC	NC	C
Sarkar et al.[11]	C	C	C	NC	C	NC	C

Fig. 1—Dogan et al.'s[9] model's prediction of bath [wt pct C] refined by emulsion zone on the basis of different droplet generation rates.

examined the effects of Si and P in the metal on decarburization reaction and developed a kinetic model based on surface blockage effect of oxides in slag. Sun et al.[16] reported that the presence of Si inhibits the decarburization rate of the metal drop, and the authors developed a kinetic model. Morales et al.[22] modified the interfacial area by considering the surface-active nature of SiO_2 to model the kinetics of FeO reduction by carbon in an EAF (Electric Arc Furnace). However, the above models are limited to only laboratory-scale results and no attempt has been made to apply this surface limiting approach for an industrial-scale converter process.

The model developed in this study is an expansion of the framework of decarburization model developed by Dogan et al.[8–10] The present model is significantly improved by incorporating several submodels such as size distribution model to account for the size of drops, surface coverage model and the modified droplet generation model. The effect of size and residence time of the droplets on decarburization efficiency of metal drop in the slag–metal emulsion was also investigated in the current study. The model's predictions were compared with the measured data of bath carbon in a 200 ton industrial converter.

II. MODEL DEVELOPMENT

The model for decarburization is based on a multi-zone kinetics approach developed by the authors in the earlier publication.[2] It has been observed that decarburization in a BOF is primarily led by the reactions in jet impact and emulsion zone. The refining of C in bath (in bulk metal and slag–bulk metal) is significantly low in comparison to the above reaction zones.[23] Therefore, in the current study, the BOF reactor has been divided into two distinctly different regimes, i.e., slag–metal–gas emulsion zone and gas–metal reaction zone in order to study the carbon refining kinetics. Decarburization rate in each zone has been computed separately and finally

combined by using mass balance equation. The concentration of carbon in the bulk metal was calculated by the following mass balance equation:

$$W_b^{t+\Delta t} \times [\text{wt pct } C_b]^{t+\Delta t} = W_b^t \times [\text{wt pct } C_b]^t - \left(\frac{dW_c}{dt}\right)_{em}$$
$$\times \Delta t - \left(\frac{dW_c}{dt}\right)_{iz} \times \Delta t + \left(\frac{dW_c}{dt}\right)_{sc} \times \Delta t$$

[2]

where W_b^t is the weight of the hot metal (kg) at time t, $W_b^{t+\Delta t}$ is the weight of the hot metal at time step $(t + \Delta t)$, pct C_b is the wt pct of C in the bulk, dW_C/dt is the decarburization rate (kg/s) and the subscripts em, iz and sc correspond to emulsion, jet impact and scrap respectively.

During the blowing process, the impurities like Si, Mn and P form their respective oxides and join the slag phase, on the other hand, C forms gaseous product (CO and CO_2). Thus the dynamic change in weight of the bulk metal has been calculated as:

$$W_b^{t+\Delta t} = W_b^t - \Delta W_m^{sl,t} + \Delta W_{sc}^{m,t} - W_m^{eject,t} + W_m^{return,t+\Delta t} - \Delta W_C^{iz,t}$$

[3]

Here $W_b^{t+\Delta t}$ is the weight of the bulk metal at time $t + \Delta t$, W_b^t is the weight of the bulk metal at time step t, $\Delta W_m^{sl,t}$ is the weight of the hot metal converts into slag (in jet impact and slag-bulk metal zone), $\Delta W_C^{iz,t}$ is the weight of carbon removed in the jet impact zone, and $\Delta W_{sc}^{m,t}$ is the weight of the melted scrap during time step Δt. $W_m^{eject,t}$ is the weight of the metal droplets ejected at time t and $W_m^{return,t+\Delta t}$ is the weight of droplet return to the bath at time $t + \Delta t$.

A. Modeling of Decarburization in the Emulsion Zone

The mechanism of bloated droplet theory has been used for estimating the rate of decarburization in slag–metal emulsion zone. The kinetics of decarburization for a single droplet in slag–metal emulsion can be described by a simple first-order rate equation in the following form[24]:

$$\frac{d[\text{wt pct } C]}{dt} = -k_d \frac{A_{app}}{V_{app}} \left([\text{wt pct } C] - [\text{wt pct } C]_{eq}\right),$$ [4]

where [wt pct C] is the weight percentage of C in the droplet, [wt pct C]$_{eq}$ is the equilibrium C percentage at slag–droplet interface, A_{app} and V_{app} are the reaction area and volume of the droplet, respectively, and k_d is the mass-transfer coefficient.

1. Microkinetics: decarburization of metal droplet in the emulsion

The "theory of bloating of droplets" was applied to evaluate the decarburization kinetics of metal droplets in the emulsion.[7] Due to bloating (or swelling) of metal droplets in emulsion, the rate parameters are continuously changing during the reaction period. The mathematical treatment to estimate the key parameters such

as residence time, droplet size, area, and volume change associated with the droplets are already discussed in the earlier publication by the authors.[1] The mass-transfer coefficient k_d was modified to take into account the surface-coverage effect of oxides in the slag.

a. Mass-transfer coefficient. Brooks *et al.*[7] assumed carbon diffusion to be the rate determining step of overall decarburization of a droplet and employed Higbie's penetration theory to estimate the mass-transfer coefficient. Since the ejected metal drops contain other impurities such as Si, Mn, and P, these elements in contact with oxidized slag form their respective oxides in the vicinity of metal–slag interface. Some of the oxides (*e.g.*, P_2O_5 and SiO_2) being surface active lower the surface tension of the slag. Also, the presence of these components can physically block the interfaces or form a viscous layer (network forming oxides), which limits the surface area available for reaction. Ideal Langmuir isotherm can describe the fraction of unoccupied sites as

$$1 - \sum \theta_c = \frac{1}{1 + \sum K_i a_i}. \quad [5]$$

Here, θ_c is the fractional adsorbed sites covered by surface-active oxides SiO_2 and P_2O_5, K_i is the adsorption coefficient of the ith species, and a_i is the activity of oxide.

For an ideal surface blockage model, the effective mass-transfer coefficient for FeO-C reaction kinetics at metal drop–slag interface due to adsorption of SiO_2 and P_2O_5, can be described as

$$k_{eff} = \frac{k_d}{1 + K_{SiO_2} a_{SiO_2} + K_{P_2O_5} a_{P_2O_5}} \quad [6]$$

The activities of SiO_2 and P_2O_5 have been calculated by the regular solution model. The adsorption coefficient K_{SiO_2} was calculated from the slope of the plot of surface tension of FeO-SiO$_2$ slag and logarithm of activity of SiO_2.[25] The detailed calculation of K_{SiO_2} has been illustrated in Appendix A1. The value of K_{SiO_2} was found to be 8.86 which is similar to the value reported by Wei *et al.*[20] The value of $K_{P_2O_5} a_{P_2O_5}$ has been taken from the relationship suggested by Hu *et al.*,[26] which is equal to 0.65 (mol pct P_2O_5) (see Appendix A2 for more details). k_d is the mass-transfer coefficient of the metal droplet in the absence of surface-active oxides, which was estimated by applying Higbie's penetration theory as described in the earlier work.[1] It should be noted that in the calculation of modified rate constant by ideal surface blockage model (in Eq. [6]), the effects of surface-active elements such as S and O in the hot metal are ignored. An empirical correlation to incorporate the effect of S on mass-transfer coefficient has been suggested in the present calculation (see Appendix B1). The authors acknowledge that due to the limited availability of experimental data, the effect of O on decarburization rate of metal droplet has been neglected in the current study.

b. Equilibrium [C] at slag–metal interface. The reaction between FeO in the slag and C in the metal droplet at the interface can be written as follows:

$$(FeO) + [C] = [Fe] + \{CO\}, \quad [7]$$
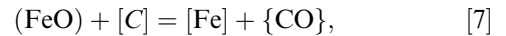
where it is assumed that the above reaction is at equilibrium at each calculation time step. Accordingly, the dynamic equilibrium concentration of carbon has been calculated by

$$[wt\ pct\ C]_{eq} = \frac{P_{CO}}{a_{FeO} \times f_c \times K_c}. \quad [8]$$

The partial pressure of CO gas was taken to be 1.52×10^5 Pa (average CO pressure inside the vessel), activity of FeO (a_{FeO}) was calculated by applying regular solution model, and the activity coefficient for carbon (f_c) was determined by an empirical correlation as a function of bath carbon concentration (see Appendix C1).[27] K_c is the equilibrium constant which is a function of temperature and derived from the standard equilibrium relation for carbon oxidation[28]:

$$\log(K_c) = 5.096 - \frac{5730}{T_m}. \quad [9]$$

2. Macrokinetics: total decarburization rate by emulsion

The total decarburization rate by the emulsion phase, in a given computational cell, has been estimated by calculating the difference between the mass of carbon ejected and the return of carbon to the bath after refining:

$$\left.\frac{dW_c}{dt}\right|_{em}^t = \frac{W_c^{eject,t} - W_c^{return,t}}{\Delta t}, \quad [10]$$

where the total amount of carbon ejects into the slag–metal emulsion at time t; $W_c^{eject,t}$ was calculated from the information of droplet generation rate and the concentration of C in the bath as

$$W_C^{eject,t} = \left(\sum_{p=1}^{P} (R_{B,T})_p^t \times \Delta t\right) \times \frac{[wt\ pct\ C]_{hm}^t}{100}. \quad [11]$$

P is the total number of divisions of the initial droplet size spectrum, $(R_{B,T})_p^t$ is the rate of droplet generated (kg/s) for a given size range at time t, and $[wt\ pct\ C]_{hm}^t$ is the concentration of carbon in the hot metal. As mentioned in the previous study,[1] the size range of ejected drops was considered to be varying between 2.3×10^{-4} and 3.35×10^{-3} m. The total size spectrum of droplets has been divided into 10 classes in the numerical calculation.

The microkinetics model estimates the final carbon concentration of the droplet at the time of its re-entry into the bath. At a given computation time, the total number of returning droplets having the final carbon concentration has been estimated, and total weight of carbon entering to the bath was calculated.

$$W_C^{return,t} = \sum_{p=1}^{P} N_p^{return,t} \times \frac{[wt\ pct\ C]_{d,p}^{return,t} \times w_{d,p}^{return,t}}{100}. \quad [12]$$

Here, $N_p^{\text{return},t}$ is the number of returning metal drops, [wt pct C]$_{\text{d,p}}^{\text{return},t}$ and $w_{\text{d,p}}$ are the concentrations of C and weight of the droplet, respectively, just before its re-entry into the molten bath at a given blowing time.

3. Modeling of decarburization rate in jet impact zone

In the jet impact zone, decarburization takes place due to oxidation of carbon in the melt with gaseous oxygen and carbon dioxide at the gas–metal interface. Based on this mechanism, Dogan et al.[10] developed a mathematical model to estimate the total rate of decarburization in the impact zone. In the current study, the model proposed by Dogan et al.[10] was applied to calculate the carbon removal rate $\left(\dfrac{dW_c}{dt}\right)_{\text{iz}}$ at each time step.

$$\left(\frac{dW_c}{dt}\right)_{\text{iz}} = \left(\frac{dW_c}{dt}\right)_{\text{iz}}^{CO_2} + \left(\frac{dW_c}{dt}\right)_{\text{iz}}^{O_2}. \quad [13]$$

In case of decarburization by CO_2, it was assumed that the rate is controlled by both mass transfer in gas phase and chemical reaction at the interface. The retracing effect of sulfur is also included in the kinetic model. The rate equation can be written as

$$\left(\frac{dW_c}{dt}\right)_{\text{iz}}^{CO_2} = -100 \times M_C A_{\text{iz}} k_a P_{CO_2}^b \quad [14]$$

where

$$k_a = \frac{1}{\frac{RT_f}{k_g} + \frac{1}{k_t}}. \quad [15]$$

Here, M_C is the molecular weight of C (g/mol). k_g, k_t, and k_a are gas phase mass-transfer coefficient, chemical reaction rate constant, and apparent rate constant, respectively. $P_{CO_2}^b$ is the partial pressure of CO_2 in gas phase, T_f is the interfacial temperature, and R is the gas constant. T_f, the gas film temperature, was defined as the mean temperature between the bulk gas and the temperature at slag–metal interface.[10] The partial pressure of CO_2 was calculated from the molar rates of gas and the average partial pressure $(P_{\text{amb}} = 1.52 \times 10^5$ Pa) inside the converter. A dynamic post combustion ratio (PCR), as already discussed in the earlier study,[1] was assumed to estimate the proportion of CO and CO_2 generated above the bath.

$$P_{CO_2}^b = \left(\frac{N_{CO_2}}{N_{CO_2} + N_{CO} + N_{\text{Ar/N}_2} + N_{O_2}}\right) \times P_{\text{amb}}, \quad [16]$$

where N represents the molar rate of the respective gas species (CO, CO_2, O_2, Ar, or N_2), and P_{amb} is the ambient pressure inside the furnace.

The rate of decarburization caused by reaction with oxygen was assumed to be controlled by mass transfer in gas phase and can be expressed by the following equation:

$$\left(\frac{dW_c}{dt}\right)_{\text{iz}}^{O_2} = -200 \times M_C A_{\text{iz}} k_g (1 + P_{O_2}^b). \quad [17]$$

$P_{O_2}^b$ in the above equation was calculated by using the similar method described in Eq. [16].

It was assumed that the rate of decarburization is controlled by mass transfer of C in the melt when the bath carbon reaches a critical value. The critical value of C has been taken to be 0.3 wt pct.[27] The rate equation can be represented by first-order kinetics as

$$\frac{dW_c}{dt} = -k_m A_{\text{iz}} \frac{\rho_m}{100} \times \left([\text{wt pct C}]_b - [\text{wt pct C}]_{\text{eq}}\right) \quad [18]$$

The jet impact area A_{iz} has been calculated assuming the shape of the area to be a paraboloid. The mass-transfer coefficient of the metal phase, k_m was estimated by the empirical relationship as a function of stirring energy proposed by Kitamura et al.[29]

4. Model formulation

The mathematical framework, assumptions, and the numerical calculation procedure for the multizone reactions in a BOF has been discussed in detail in the earlier study.[1] In the case of decarburization reaction, the sequence of calculation of overall refining rate obtained from jet impact and slag–metal emulsion zone are illustrated in Figure 2.

The slag generation model simultaneously estimates the dynamic evolution of slag chemistry and acts as an
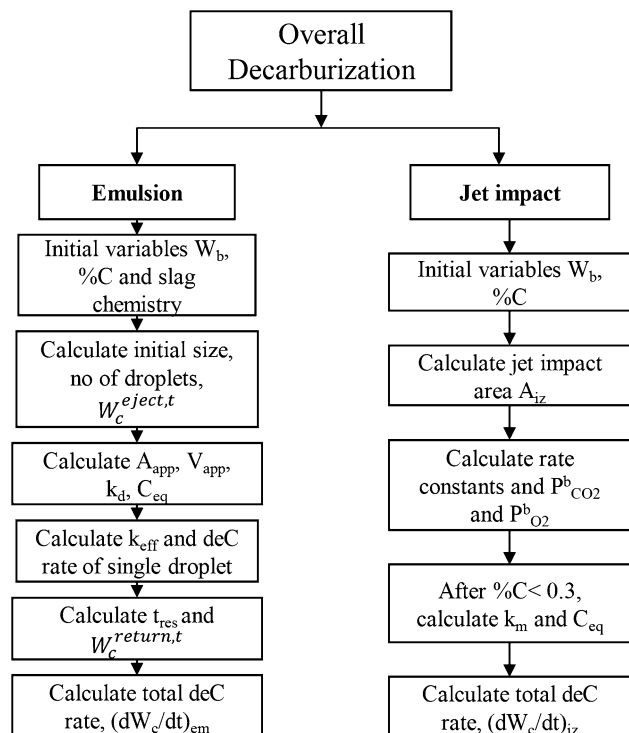

Fig. 2—Algorithm for overall decarburization rate estimated from two reaction zones.
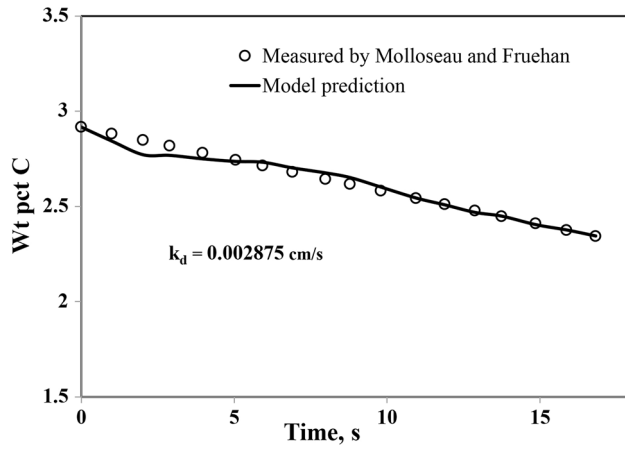
Fig. 3—Estimation of mass-transfer coefficient of C for Fe-C-S droplet.

Fig. 4—Modeling of decarburization kinetics of Fe-C-Si droplets in slag.

input to the decarburization model at each numerical time step.[1] The various submodels like the calculation of jet penetration area, droplet generation rate, and residence time were connected in parallel to compute the transient change in the rate parameters for the evaluation of the decarburization rate in each zone.

III. RESULTS AND DISCUSSIONS

A. *Decarburization Kinetics of Fe-C-Si Droplet in Slag*

Molloseau and Fruehan[6] measured the decarburization rate of Fe-C-S droplet when it passes through FeO-CaO-SiO$_2$-MgO-type slag. Considering that the decarburization kinetics follows first-order rate equation, mass-transfer coefficient was evaluated by fitting the measured C in Eq. [4] by the least square approach. Figure 3 shows the first-order rate equation fitted with the experimentally measured data by Molloseau for 10 wt pct FeO in slag. The best-fitted value of mass-transfer coefficient was found to be 0.002875 cm/s (R^2 = 0.97).

In another study by Sun et al.,[30] the kinetics of decarburization was measured for Fe-C-Si-Mn droplets in FeO-CaO-SiO$_2$-Al$_2$O$_3$-type slag. A comparative study has been performed to observe the effects of Si and Mn on the decarburization rate of the metal drop. Figure 4 shows the comparison between the rate of decarburization for Fe-C-S droplets and that of Fe-C-Si-Mn droplet reported by Sun et al. The solid line shows the model's prediction of decarburization with the mass-transfer coefficient derived from the data given by Molloseau et al. It was observed that the rate of decarburization in the presence of Si slows down the decarburization, a conclusion in agreement with several researchers.[18,20,30] In order to simulate the effect of Si on the decarburization rate, we have applied the surface coverage model due to SiO$_2$ in the slag, and the effective mass transfer can be written as

$$k_{eff} = \frac{k_d}{1 + 8.86 a_{SiO_2}} \qquad [19]$$

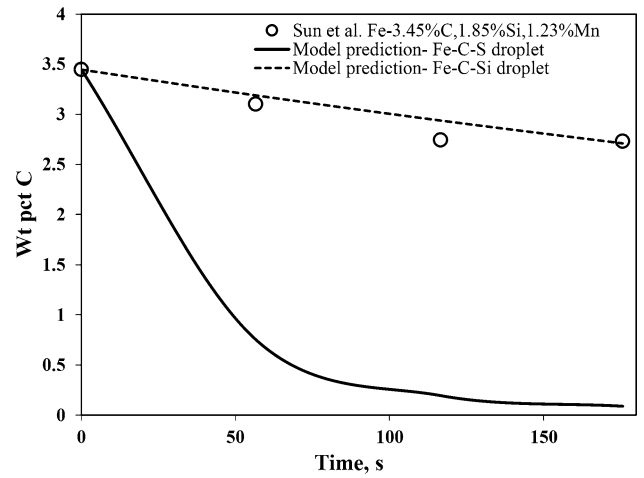The dotted line in Figure 4 is the predicted decarburization rate calculated by applying Eq. [19] at the slag–metal interface. As seen in the figure, an excellent agreement has been found between the model's prediction and the measured value of carbon concentration, which shows that the observed slow decarburization kinetics in the presence of high Si in the droplet can be explained by surface-adsorption effect of SiO$_2$ described by the modified mass-transfer coefficient obtained by Eq. [19].

B. *Decarburization Efficiency of a Metal Droplet in Emulsion*

The following equation can express the decarburization efficiency of a metal droplet during a single metal circulation period (from the time of ejection from the melt to the time when it returns to the bulk metal):

$$\eta_c(pct) = \frac{C_{p,o}^t - C_{p,r}^{t+t_{res}}}{C_{p,o}^t} \times 100, \qquad [20]$$

where η_c is the efficiency of C removal for the droplet of size class p, $C_{p,o}^t$ and $C_{p,r}^{t+t_{res}}$ are the concentrations of carbon (wt pct) in the droplet at the time of ejection from the melt and the time of return to the bulk metal, respectively.

Figure 5 shows the decarburization efficiency profile of the metal droplets as a function of its diameter during the different blowing periods of blowing. As seen from the figure, the droplets in the lower region of the size spectrum exhibit a higher value of efficiency compared with the bigger droplets. A similar observation has been reported by Millman et al., suggesting that the small-sized droplets decarburize strongly compared with the larger-sized droplets.[5] By examining the metal samples in the emulsion collected from a real converter, Cicutti et al.[4] also reported that the decarburization efficiency of a metal drop is a strong function of the size of droplets. The smaller-sized droplets ($\leq 5 \times 10^{-4}$ m) can achieve more than 80 pct of carbon refining by emulsion. A similar observation was made by Millman
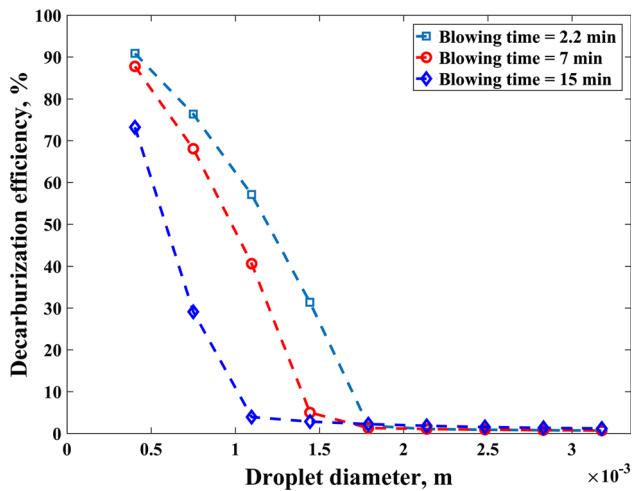
Fig. 5—Decarburization efficiency of a metal droplet as a function of droplet size.

Fig. 6—Residence time prediction of the metal droplets in slag as a function of blowing time.

et al.[5] in a 6-ton pilot-scale converter. It was observed that apart from strong decarburization, the concentrations of other elements such as P, Mn, and V are extremely low for a droplet of the size of the order 0.1 mm (~ 10^{-4} m). The numerical predictions obtained from the current study also find similar observations. For droplets having an initial size of 0.4 mm (4×10^{-4} m), the efficiency decarburization was observed to be as high as 90 pct. As the size of metal drops increases, the refining efficiency gradually decreases. Accordingly, the model predicts that in order to achieve high decarburization efficiency, the initial size of the ejected droplets should not exceed a certain order of magnitude. This behavior can be explained by analyzing the residence time of the metal drops in the emulsion phase.

The residence time of a droplet in the slag–metal emulsion can be related to the ability of metal droplet to remain buoyant. Dogan et al.[9] reported that the residence time of the metal droplets having high carbon concentration exhibits longer residence time in the emulsion regardless of their initial size. This conclusion can be true for Fe-C droplets. However, in the presence of Si, Mn, and P in the metal, the rate of CO nucleation inside the drop either delays or decreases and can certainly affect the droplet-swelling process. Figure 6 shows the calculated residence time of a Fe-C-Si-Mn-P metal droplet by applying the surface blockage model. It is interesting to observe that the residence time of the droplets increases with the increasing diameter of the droplet to a certain size and then decreases during the initial part of the blow. However, the droplets in the lower-size spectrum exhibit longer residence time compared with larger-sized ones during the second stage of blow (~ after 7 minutes). Further, it was observed that the ejected droplets mean diameter of which is more than 1.4 mm (1.4×10^{-3} m) are incapable of bloating and thus return to the bath immediately, which results in significant reduction of carbon refining in the molten metal. Figure 6 shows the predicted residence time as a function of the blowing time, which is a complex
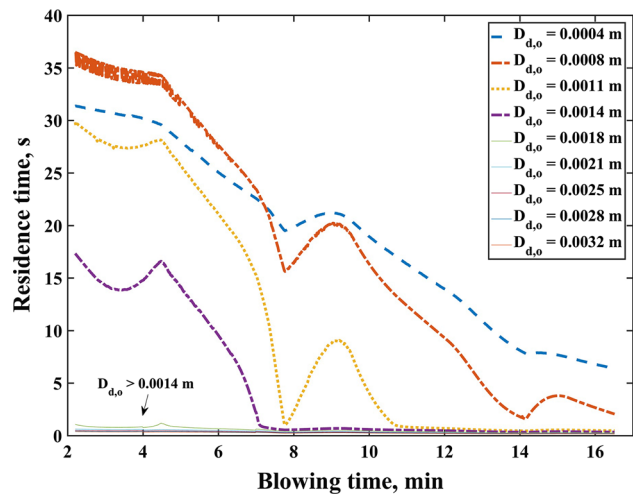
function of lance height, slag FeO, C concentration, and decarburization rate in the bulk metal. A sudden change in the predicted residence time profiles at the 4th and 7th minutes is primarily caused by change in lance height during the blowing operation.

The residence time behavior of the metal droplets for small droplets can be explained qualitatively by analyzing the mechanism of swelling of droplets in the slag–metal emulsion. Chen and Coley[17] show that swelling will only occur if CO bubble nucleates before the metal droplets return back to the metal phase. The study indicated that the total time of flight (ascending–bloating–descending) of the dense droplets should be more than the incubation time for nucleation of CO gas, which is illustrated in Figure 7. The incubation time for bloating is a strong function of carbon concentration and FeO in slag, and it sharply increases with the decreasing carbon concentration. The competition between incubation time for CO nucleation and time of flight of the dense droplet will decide the occurence of bloating (or swelling).

In line with the experimental evidence by Molloseau et al.,[5] modeling results by Brooks et al.[7] and Dogan et al.[9] suggested that large drops exhibit long residence time due to the presence of high carbon concentration. However, these observations are based on Fe-C-S metal drops, and the retarding effects of Si, Mn, and P on bloating process were not considered. As reported by Sun et al.,[16] in the presence of Si, Mn, and P in the melt, the decarburization kinetics reduces significantly. The nucleation of CO bubbles becomes easier for small-sized droplets having high carbon and slag containing high concentration of FeO. It may be due to the large value of surface area to volume ratio (A_{app}/V_{app}) and the mass-transfer coefficient associated with small-sized drops ($k_d \propto 1/d_{drop}$), which enhance the decarburization rate to reach the threshold level for bloating in a quicker period of time. Once these droplets become buoyant in emulsion, the remaining carbon can facilitate the nucleation process and hence can increase the residence time. This behavior is seen in Figure 6, where
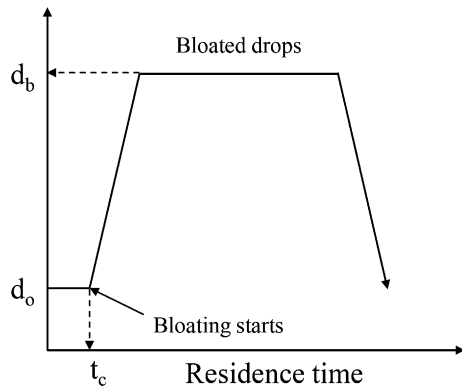
Fig. 7—Qualitative representation of the mechanism of bloating of metal drops in slag.

Fig. 8—Decarburization rate by emulsion calculated by the model.

the residence time is predicted to be reaching a maximum value for 0.8 mm (8×10^{-4} m) diameter droplets during initial blowing period (< 7 minutes). After approximately 7 minutes of the blow, the lower-sized droplets were observed to exhibit high residence time in slag. Large drops having diameter more than 1.4 mm (1.4×10^{-3} m), on the other hand, spend only a fraction of second in the emulsion. The reason for this small residence time may be the slow rate of decarburization associated with the large diameter drops that failed to achieve the threshold decarburization for the initiation of bloating process during the flight time in the emulsion.

C. Decarburization Rate in Emulsion

Overall decarburization rate in the emulsion zone was computed by summing the weight of carbon removed from all the individual metal droplet in the emulsion at each computational time step. Figure 8 shows the overall carbon refining in the metal droplets in the slag–metal zone as a function of blowing time. It was observed that during the initial part of the blow (< 4.5 minutes), the overall refining rate of carbon due to the slag–metal emulsion is considerably low, *i.e.*, the predicted decarburization rate falls below 1 kg/s. The low rate of decarburization can be explained by the amount of droplets present in the emulsion and the kinetics of reaction during the initial part of the blowing process. During the first few minutes of the process, the lance height is kept at a higher position which leads to less number of metal droplets ejected into the emulsion. Also, the early formation of SiO_2 and P_2O_5 in the slag, the kinetics of decarburization slows down due to occupancy of these oxides at the interface of the metal drop, decreasing the effective surface area for carbon oxidation. In Cicutti's heat data,[4] which has been used for this modeling work, the initial lance height was kept at 2.5 m until 4 min of the blow and afterward, it was reduced to 2.2 m. It should be noted that with the decrease of 0.3 m in height of the lance, the amount of droplets ejected can increase from 361 kg/s to more than 1000 kg/s. The increase in the amount of ejection of me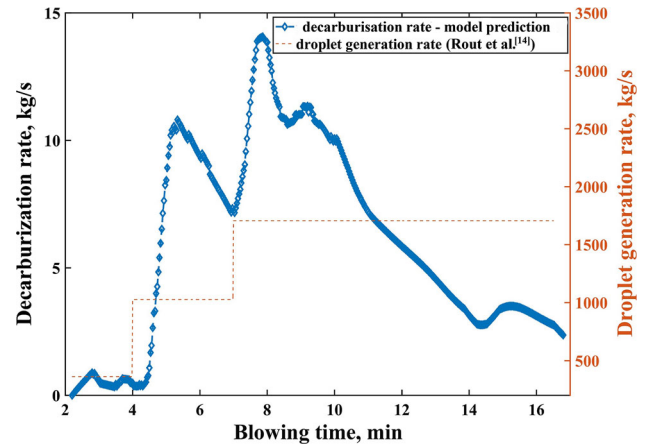tal droplets into the emulsion can enhance the rate of refining. Thus, it appears that the sudden increases in the rate at blowing times of 4 and 7 minutes are the result of a large number of droplets being ejected into the emulsion. However, it was observed that at a constant lance position, the rate decreases after it reaches a peak value (from 6 to 7 and from 8 to 16 minutes). This behavior is due to the decrease in the residence time of the metal droplets as a result of decreases in melt carbon concentration and FeO in the slag.

The present model calculation result shows that the peak value of decarburization occurs at about 8 minutes after the start of blowing. This finding is consistent with the measured data of C concentration in the bath, which shows that the peak decarburization occurs between 6 and 11 minutes of the blowing time. Further, the total carbon removed by the emulsion has been computed by estimating the area under the curve of decarburization rate and blowing time. The calculation shows that 5200 kg of carbon has been removed by emulsion zone, which accounts for nearly about 76 pct of the total carbon refining during the entire blowing period. The slight increase in decarburization rate during the last stage of blowing (from 14 to 15 minutes) is due to increase in residence time of the droplets (0.8 mm drops as seen from the Figure 6) as a result of increase in the predicted FeO in the slag.

D. Decarburization in Impact Zone

The Eq. [13] has been applied to compute the decarburization rate from the impact zone at each numerical time step. Figure 9 shows the decarburization rate predicted by the model in the jet impact zone. It was observed that the rate of carbon removal in the impact zone is primarily driven by a change in lance height in the blowing region when the carbon concentration in the bath is more than a critical value. In this region, the carbon oxidation is controlled by oxygen diffusion into the melt, and low lance height favors the kinetics of the reaction by creating a large gas–metal interfacial area. The present model's estimation shows that changing the lance height from 2.5 to 1.8 m can improve the
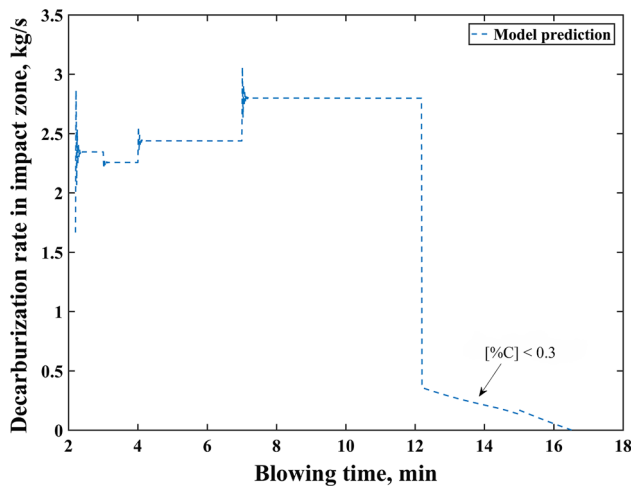
Fig. 9—Model's prediction of decarburization rate in impact zone.

Fig. 10—Model's prediction of C wt pct in bath and its comparison with measured data.

decarburization rate from 2.43 to 2.8 kg/s. Once the carbon reaches a threshold carbon concentration in the bath, the rate is limited by mass transport of carbon in the melt. In the current study, a fixed value of critical carbon concentration of 0.3 wt pct has been used for the model calculation. The calculated decarburization rate is below 0.5 kg/s during this domain, and it is observed to decrease with the decreasing bath carbon concentration.

The area under the decarburization rate *vs* blowing time profile was calculated by using trapezoid rule, and the total amount of carbon removed from the impact zone was estimated. The predicted result shows that approximately ~ 24 pct of C (total about 1607 kg) of total carbon has been withdrawn by the jet impact zone during the entire blowing period.

E. *Overall Decarburization in Bath*

The model's prediction of carbon concentration in the bath as a function of blowing time is shown in Figure 10. As seen from the figure, the model's prediction agrees well with the industrially measured data of Cicutti et al.[4] The slow rate of decarburization reaction during the early part of the blowing process is well captured by the proposed surface-limiting model. The three distinct regions can be observed from the model's prediction of C in the bath, which is usually experienced in many decarburization profiles reported in the literature.

Region I The rate of decarburization was observed to be weak during first 4.5 minutes of blowing time. The decarburization rate in this period is calculated to be 0.156 wt pct/min. The weak decarburization in this period is due to the ejection of a less number of droplets and the slow decarburization kinetics of metal drops due to the presence of surface-active oxides.

Region II A constant rate of decarburization was observed between 4.5 and 12 minutes of blowing time. In this region, the lance height operates in the lowest position. That means a significant number of drops enter into the emulsion phase. Further, the kinetic restriction
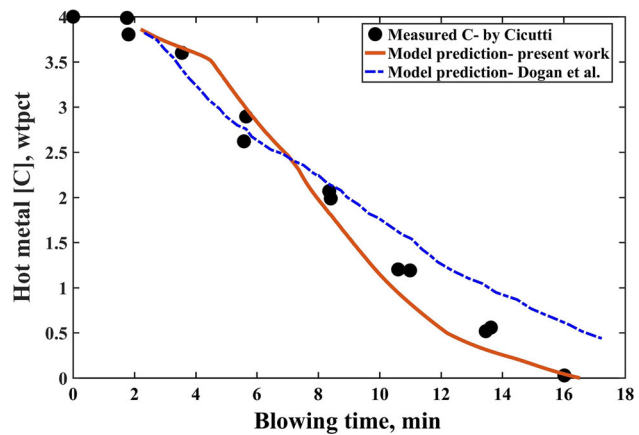
due to reduction of interfacial area has been leveraged as the surface-active oxides start to dissolve in the slag and no longer creates a barrier for the decarburization reaction at the interface. Thus, the rate of decarburization proceeds with full speed in this region. The rate is estimated to be approximately 0.25 wt pct/min. This value can be comparable with the peak decarburization of 0.3 wt pct /min reported by Cicutti et al.

Region III The decarburization rate was further observed to decrease to a lower value after 12 minutes of the blow, once it reaches the critical carbon content in the bath. In this region, the rate of decarburization in the impact zone drastically decreases. However, some amount of refining by the emulsion zone was noticed for small-sized droplets.

Compared with the previous model's prediction by Dogan *et al.*,[8–10] the present model gives a better insight into carbon refining in a BOF, particularly during the initial and final parts of the blow period. The slightly overprediction of decarburization rate obtained from Dogan *et al.'s* model during the early part of the blow may be because the model did not take into account the competitive kinetics of other elements such as Si and P in the melt. Similarly, the weak decarburization rate predicted by Dogan's model during the end of blow period is due to the low prediction of refining rate by emulsion zone. It was therefore evident that a single size of droplets cannot represent accurately the kinetics of reactions in the emulsion.

IV. CONCLUSIONS

A multizone kinetic model has been established and used to simulate the decarburization rate of a top blowing steelmaking process. A significant improvement in the previous kinetic model developed by Dogan *et al.* was achieved by incorporating the adsorption effect of surface-active oxides, the size distribution of initial droplets and modified droplet generation rate in the mathematical formulation in the emulsion zone of carbon refining. By combining this with the rate model for decarburization by the impact zone, the overall rate

of carbon removal from the bulk metal was simulated. The model's predictions were validated with industrial data reported by Cicutti et al.,[4] and an excellent agreement has been found. Based on the present study, the following conclusions can be drawn:

1. It was predicted that surface-active oxides like SiO_2 and P_2O_5 in the slag are responsible for inhibiting the decarburization kinetics in emulsion particularly during the early blow period by blocking the interfacial sites for reaction. A classical surface coverage model can be suitable for studying decarburization kinetics in a multicomponent slag system.
2. The decarburization rate in the emulsion is predicted to be sensitive to the size of the droplet ejected from the melt. Not all the droplets ejected into the emulsion zone are participating in the reaction, only those drops which are able to bloat can only participate in effective emulsion–carbon conversion process. The present model's prediction shows that only droplets having an initial diameter of less than 1.4 mm (1.4×10^{-3} m) are responsible for carbon refining by slag–metal emulsion.
3. The decarburization efficiency of a metal drop in emulsion is predicted to be dependent on the initial size and carbon concentration. Generation of fine metal drops with higher carbon contents is predicted to be the favorable conditions for achieving high decarburization rate in the emulsion phase.

ACKNOWLEDGMENT

APPENDIX A

A1 Calculation of Adsorption Coefficient K_{SiO_2}

Combining Gibbs isotherm with that of Langmuir, the surface tension of FeO-SiO$_2$ slag system can be expressed by the following equation:

$$\sigma = \sigma_0 - RT\Gamma^0_{SiO_2} \ln(1 + K_{SiO_2} a_{SiO_2}), \qquad [A1]$$

where $\Gamma^0_{SiO_2}$ is the saturation concentration of adsorbed SiO_2, K_{SiO_2} is the adsorption equilibrium constant, and a_{SiO_2} is the activity of SiO_2. σ is the surface tension of the FeO-SiO2 melt, and σ_0 is the surface tension of SiO_2-free iron oxide melt. The above equation can be rearranged in the form of a linear equation as $y = mx$, where $y = \exp\left(\frac{\sigma_0 - \sigma}{RT\Gamma^0_{SiO_2}}\right) - 1$ and $x = a_{SiO_2}$. The plot of y vs x is shown in Figure A1. The saturation concentration $\Gamma^0_{SiO_2}$ was taken to be 6.55×10^{-10} mole/cm^2 from the surface tension data proposed by Richardson et al.[31] The value of K_{SiO_2} was calculated to be 8.86 from the slope of the plot in Figure A1. Similar value of adsorption coefficient of SiO_2 was reported by Wei et al.[21] for FeO-SiO$_2$ slag system.
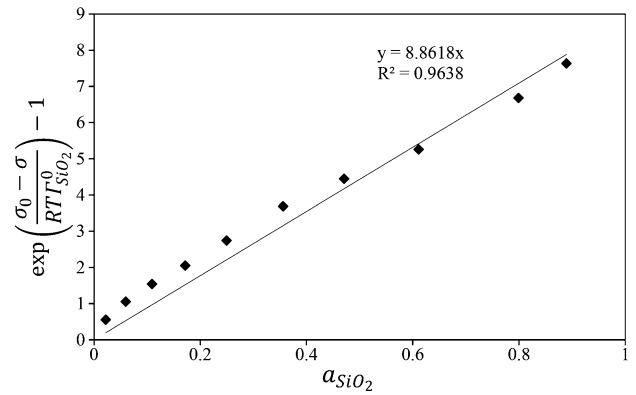

Fig. A1—Calculation of K_{SiO_2} from surface tension data.

A2 Calculation of Adsorption Coefficient $K_{P_2O_5}$

The slag containing P_2O_5 can interfere with the FeO adsorption on the slag–metal interface and thus can retard the decarburization rate. Hu et al.[26] reported that the for FeO_x-P_2O_5 melts, the activity of P_2O_5 follows Henry's law when the concentration of P_2O_5 falls below 8 mole pct. The fraction of occupied sites of P_2O_5 at the interface according to Hu et al.[26] is defined as

$$\theta_p = \frac{0.65 \text{ (mole pct } P_2O_5)}{1 + 0.65(\text{mole pct } P_2O_5)} \qquad [A2]$$

From Eq. [A2], the value of $K_{P_2O_5} a_{P_2O_5}$ is assumed to be 0.65(mole pct P_2O_5) in the current study.

APPENDIX B

B1 Effect of S on Decarburization Rate

Several studies indicated that the presence of S in the iron droplet influences the rate of decarburization by FeO in the slag. Sulfur is a highly surface-active element in liquid iron, and it can affect the decarburization rate in two ways: (i) segregating at the interface and limiting the interfacial area by blocking the reaction sites; and (ii) decreasing the slag–metal interfacial tension and making it easier for emulsification (enhances the interfacial area). Since the rate of reaction is directly proportional to the reaction area, the competition between the positive effect of emulsion formation and the negative effect of surface blockage has been observed. Molloseau et al.[6] observed that decarburization reaches a maximum value when $S = 0.011$ wt pct and any further increase in S decreases the reaction rate. Similar observation was made by Chen et al.,[17] and this value has been reported to be 0.013 wt pct. The total interfacial area evolution for Fe-C-S droplets in slag is a combination of both bloating due to CO nucleation and emulsification due to the presence of S.

$$\text{Total interfacial area} = A_{\text{bloating}}(\text{CO}) + A_{\text{emulsification}}(\text{S}) \qquad [B1]$$

Modeling of interfacial reaction area due to the effect of S in the iron droplet is complex. The decrease in surface area due to adsorption of S at the interface can
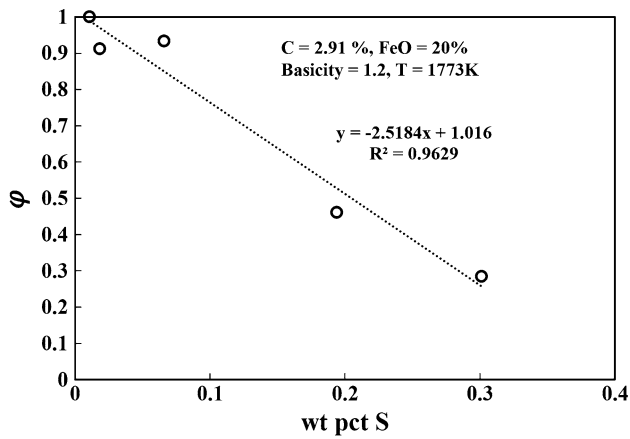
Fig. B1—Rate constant-modified parameter as a function of S in the metal droplet. Reproduced with permission from Molloseau et al.[6] and Chen et al.[17]

be described by means of surface blockage mechanism. However, it is difficult to distinguish between the surface area change due to CO nucleation and emulsification by surface-active elements such as S. In the model proposed by Brooks et al.,[7] the total change in interfacial area of the metal droplet has been empirically correlated with decarburization rate and slag FeO. The correlation was developed on the basis of Fe-C-0.011S data, where the rate of decarburization is observed to be at peak value. This method of calculation of interfacial area can be considered as standard state, and for high concentration of sulfur ($S > 0.011$ wt pct), decarburization rate can be calculated by the correcting the interfacial area with respect to the standard state. For application of Brooks et al.'s model for high S concentration, we defined a rate constant modified as

$$\varphi = \frac{\text{Rate of decarburization}}{\text{Maximum rate of decarburization observed at } S = 0.011\text{wt pct}},$$
[B2]

where $\varphi = 1$ means the rate of decarburization reaches the maximum value due to large increase in surface area caused by S. At higher S level, φ is less than 1 due to the surface blocking effect of S on reaction interface.

At high S level in the steel, the decarburization rate must be multiplied by the rate constant-modified parameter to get the actual rate due to the effect of sulfur. The experimental data by Molloseau et al. and Chen et al. have been used, and φ as a function of S in the droplet is plotted in Figure B1.

For $S > 0.011$ and < 0.3 wt pct

$$\varphi = 1.016 - 2.5184 \times [\text{wt pct S}]$$
[B3]

$$k_{\text{eff}}^{s} = k_{\text{eff}} \times \varphi$$
[B4]

It should be noted that due to lack of experimental data, the empirical equation derived for φ is simplistic in nature, and it has been derived at constant C, slag FeO, and

temperature. In Cicutti's heat data used for the present model's calculation, S concentration is about 0.015 wt pct. The modified rate parameter φ corresponds to this S level which is estimated to be 0.96 in the current study.

APPENDIX C

C1 Activity Coefficient of C

The activity coefficient of C was calculated by the following relationships[27]:

$$a_C = [\text{Pct C}]f_c$$
[C1]

$$\log f_c = 0.1666[\text{Pct C}] - 0.01585[\text{Pct C}]^2 + 9.9613 \\ \times 10^{-7}[\text{Pct C}]^3(T - 273) \\ + 3.0246 \times 10^{-5}[\text{Pct C}](T - 273)$$
[C2]

NOMENCLATURE

a_i	Thermodynamic activity (–)
A_{app}	Apparent area of the droplet (m²)
C_b	Carbon concentration in bulk metal (wt pct)
C_{eq}	Equilibrium carbon concentration (wt pct)
D_c	Diffusion coefficient of carbon (m²/s)
d	Diameter of droplet (m)
dW_C/dt	Decarburization rate (kg/s)
k_d	Mass-transfer coefficient of decarburization of a droplet (s⁻¹)
k_{eff}	Effective mass-transfer coefficient with surface blocking effect (s⁻¹)
K_{SiO_2}	Adsorption coefficient of SiO₂ (–)
$K_{\text{P}_2\text{O}_2}$	Adsorption coefficient of P₂O₅ (–)
P_{amb}	Ambient pressure inside furnace (Pa)
p	Class in droplet size spectrum (–)
r_c	Decarburization rate of droplet (wt pct/s)
r_c^*	Critical decarburization for bloating (wt pct/s)
u	Velocity of droplet (m/s)
V_{app}	Apparent volume of the droplet (m³)
W_b	Weight of bulk metal (kg)
W_c	Weight of carbon (kg)
W_{sc}	Weight of scrap added (kg)
W_m^{sl}	Weight of metal in slag (kg)
W_m^{eject}	Weight of metal ejected (kg)
W_m^{return}	Weight of metal return to the bath (kg)
W_{slag}	Weight of slag (kg)
W_{lime}	Weight of lime dissolute into slag (kg)

GREEK SYMBOLS

θ_c	Fraction of occupied sites due to surface-active oxides (–)
ρ_d	Density of droplet (kg/m³)
$\rho_{d,0}$	Initial density of droplet (kg/m³)
σ	Surface tension (N/m)

Γ^0 Saturation concentration of adsorbed species (mole/cm^2)

η Efficiency of decarburization (–)

SUBSCRIPTS/SUPERSCRIPTS

em   Emulsion zone
iz   Impact zone
deC   Decarburization

REFERENCES

1. B.K. Rout, G. Brooks, M.A. Rhamdhani, Z. Li, F. Schrama, and J. Sun: *Metall. and Mater. Trans. B*, 2018, vol. 49B, pp. 537–57.
2. P. Kozakevitch: *Journal of Metals*, 1968, vol. 22, pp. 57–67.
3. H.W. Meyer, W.F. Porter, G.C. Smith, and J. Szekely: *J. Metals*, 1968, vol. 20, pp. 35–42.
4. C. Cicutti, M. Valdez, T. Pérez, J. Petroni, A. Gómez, R. Donayo and L. Ferro: In *Sixth International Conference on Molten Slags, Fluxes and Salts*, ISS, ed., Stockholm-Helsinki, Warrandale, PA, 2000.
5. M.S. Millman, A. Kapilashrami, M. Bramming and D. Malmberg: European Union, Luxembourg, 2011.
6. C.L. Molloseau and R.J. Fruehan: *Metall. Mater. Trans. B*, 2002, vol. 33B, pp. 335–44.
7. G. Brooks, Y.H. Pan, D. Subagyo, and K. Coley: *Metall. Mater. Trans. B*, 2005, vol. 36, pp. 525–35.
8. N. Dogan, G.A. Brooks, and M.A. Rhamdhani: *ISIJ Int.*, 2011, vol. 51, pp. 1086–92.
9. N. Dogan, G.A. Brooks, and M.A. Rhamdhani: *ISIJ Int.*, 2011, vol. 51, pp. 1093–1101.
10. N. Dogan, G.A. Brooks, and M.A. Rhamdhani: *ISIJ Int.*, 2011, vol. 51, pp. 1102–09.
11. R. Sarkar, P. Gupta, S. Basu, and N.B. Ballal: *Metall. Mater. Trans. B*, 2015, vol. 46B, pp. 961–76.
12. D. Subagyo, G.A. Brooks, K.S. Coley, and G.A. Irons: *ISIJ Int.*, 2003, vol. 43, pp. 983–89.
13. B.K. Rout, G.A. Brooks, M.A. Rhamdhani, and Z. Li: *Metall. Mater. Trans. B*, 2016, vol. 47B, pp. 3350–61.
14. S.C. Koria and K.W. Lange: *Metall. Trans. B*, 1984, vol. 15B, pp. 109–16.
15. Q.L. He and N. Standish: *ISIJ Int.*, 1990, vol. 30, pp. 305–09.
16. H. Sun: *ISIJ Int.*, 2006, vol. 46, pp. 1560–69.
17. E. Chen and K.S. Coley: *Ironmak. Steelmak.*, 2010, vol. 37, pp. 541–45.
18. E.W. Mulholland, G.S.F. Hazeldea, and M.W. Davies: *J Iron Steel*, 1973, vol. 211, pp. 632–39.
19. D.E. Woolley and U.B. Pal: In *58 th Ironmaking Conference*, 1999, pp 413–29.
20. W.M. Kim, G. Granzdorffer, and H. Fine: *Steel Res.*, 1988, vol. 60, pp. 166–70.
21. W. Pan, M. Sano, M. Hirasawa, and K. Mori: *ISIJ Int.*, 1991, vol. 31, pp. 358–65.
22. R.D. Morales, H. Rodríguez-Hernández, P. Garnica-González, and J.A. Romero-Serrano: *ISIJ Int.*, 1997, vol. 37, pp. 1072–80.
23. D.J. Price and M.J. Jones: *Process Engineering of Pyrometallurgy Symposium*, 1974.
24. G.A. Brooks, M.A. Rhamdhani, K.S. Coley, D. Subagyo, and Y. Pan: *Metall. Mater. Trans. B*, 2008, vol. 40B, pp. 353–62.
25. Y. Chung and A. Cramb: *Metall. Mater. Trans B*, 2000, vol. 31B, pp. 957–71.
26. X. Hu, H. Matsuura, and F. Tsukihashi: *Metall. Mater. Trans. B*, 2006, vol. 37B, pp. 395–401.
27. K. Chou, U.B. Pal, and R.G. Reddy: *ISIJ Int.*, 1993, vol. 33, pp. 862–68.
28. E.T. Turkdogan: *Fundamentals of steelmaking*, The Institute of Materials, London, 1996, p. 182.
29. S. Kitamura, T. Kitamura, K. Shibata, Y. Mizukami, S. Mukawa, and J. Nakagawa: *ISIJ Int.*, 1991, vol. 31, pp. 1322–28.
30. Honglei Sun and Guangqing Zhang: *ICS Proceeding*, 2005, pp 257–68.
31. F.D. Richardson: *Phys. Chem. Melts Metall.*, 1974, vol. 2, p. 441.